Detwiler, P.O. and Nagurka, M.L., "Track Geometry Modeling for Rail Vehicle Studies," Dynamic Systems: Modelling and Control, *ed.* Donath, M., ASME DSC-Vol. 1, 1985, pp. 325-331.

TRACK GEOMETRY MODELING FOR RAIL VEHICLE STUDIES

P. O. Detwiler and M. L. Nagurka
Department of Mechanical Engineering
Carnegie-Mellon University
Pittsburgh, PA 15213

ABSTRACT

This paper discusses a general model of track geometry for rail vehicle dynamic simulation studies. The model characterizes both deliberate track changes, such as track curvature and superelevation, and unintentional changes due to track irregularities. The deliberate track changes represent inputs which permit the simulation of the dynamic response of vehicles during curve entry, negotiation, and exit. The unintentional variations are used to model stochastic track inputs, such as alignment, gauge, and crosslevel irregularities, and to represent deterministic inputs due to rail joints and other phenomena. The general track model is coupled with a vehicle dynamic curving simulation routine that can be used to study the performance of vehicles with different suspension designs and wheel profiles operating on a variety of track environments. Here, selected simulation results of vehicle dynamic response due to track geometry variations are presented.

NOMENCLATURE

a	half of track gauge
A	roughness parameter
b	half of wheelbase
D	degree curve
g	acceleration due to gravity
H	transfer function
k_{b2}	interaxle bending stiffness
k_{px}	primary longitudinal suspension stiffness
k_{py}	primary lateral suspension stiffness
k_{s2}	interaxle shear stiffness
P	power
R	curve radius
s	Laplace variable
S	power spectral density
v	cutoff frequency
V	vehicle forward speed
X_s	step size
y	spatial representation of irregularity
Y	frequency domain representation of irregularity
Δy	cant deficiency steering offset
$\Delta\psi$	track curvature steering offset
μ	mean
σ	standard deviation (square root of variance)
φ_d	cant deficiency
φ_{se}	track superelevation angle

Conversion Factors

1 deg	=	0.01745 rad
1 ft = 12 in	=	0.3048 m
1 lb	=	4.448 N
1 mph	=	0.4470 m/sec

INTRODUCTION

One of the most important and often overlooked components of the rail vehicle dynamic system is the track itself. The track geometry represents a system input that influences vehicle dynamic behavior. Studies of vehicle performance and, in particular, wheelset response, require a proper model of the track geometry.

This paper discusses a general model of track geometry. The model is an important tool which can be coupled with vehicle simulation routines to study the performance of different vehicle designs running on a variety of track environments. The track geometry model, which includes both deliberate and unintentional variations, is developed in detail below. The deliberate track changes represent inputs which permit the simulation of the dynamic response of vehicles during curve entry, negotiation, and exit. The unintentional variations are used to model stochastic track inputs, such as alignment, gauge, and crosslevel irregularities, and to represent deterministic inputs due to rail joints and other phenomena.

Particular attention has been paid to stochastic irregularities, which are determined from power spectral density information and are modeled as stationary, ergodic, Gaussian, random processes. Due to their stochastic nature, the irregularity data are viewed as a set of random processes with known statistics (means, variances, and power spectral densities). Where appropriate, various vehicle output data (state trajectories and performance indices) are also treated as random processes.

The influence of geometric track variations on vehicle transient response is studied using a computer simulation model that describes the lateral dynamics of rail transit vehicles during tangent and curved track negotiation. The computer model includes nonlinear effects due to wheel/rail profile geometry, wheel/rail creep force saturation, and piecewise-linear suspension elements. In addition, the model can represent a variety of truck suspension designs and can account for single-point and two-point wheel/rail contact. In this paper, a brief description of the rail vehicle dynamic simulation model is provided. The vehicle and track geometry models are combined, and are used to demonstrate the influence of track geometry inputs on vehicle dynamic response.

Literature Review

Analytical descriptions of unintentional variations in track geometry were reported by Hamid, *et al.* [1]. However, the descriptions in [1] do not include methods to generate irregularity data for vehicle studies. Arslan [2] modeled tangent track random irregularities (alignment and crosslevel)[1] as input to a nonlinear rail vehicle model and described a means to generate these irregularities. Dzielski [3] studied the effects of alignment and crosslevel irregularities on energy dissipation in a model of freight car curve negotiation. Both researchers [2, 3] neglected deterministic, gauge, and surface irregularities. Nagurka [4] developed a dynamic curving model of a rail transit vehicle that includes track curvature and superelevation, but neglects rail irregularities. A description of his model and selected performance results are presented in [5].

Scope of Paper

This paper is an attempt to combine a complete description of alignment, gauge and crosslevel irregularities (deterministic and random) with a model of track curvature and superelevation. This general track geometry model is used as input to a nonlinear rail vehicle model and limited results of simulation studies are reported.

TRACK GEOMETRY VARIATIONS

Variations in track geometry as a function of distance along the track represent significant inputs to the rail vehicle dynamic system. These geometry variations may be classified, in a broad sense, into those that are deliberate and those that are unintentional. Deliberate variations include track curvature, superelevation, and grade. Unintentional variations may be thought of as track errors, and are commonly referred to as rail irregularities.

The two classes of track geometry variations are distinct in more than a causal sense. Deliberate changes are, in general, of large magnitude and low (spatial) frequency, while rail irregularities are typified by small amplitude and high (spatial) frequency.

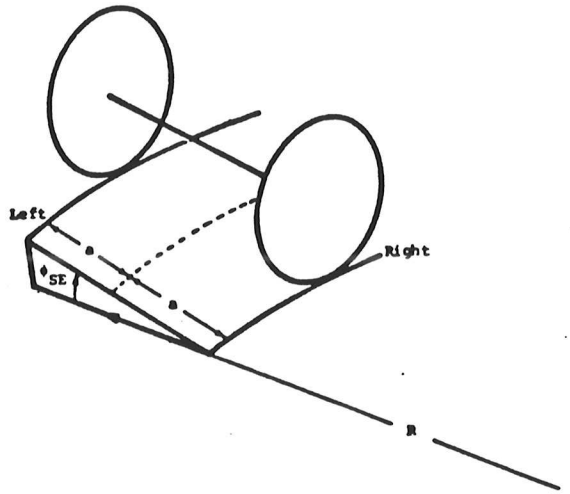

Figure 1: Definitions of Radius of Curvature and Superelevation Angle.

Deliberate Variations

In this paper, two types of deliberate track geometry variations are considered: track curvature and superelevation. Track curvature is defined as 1/R, where R is the curve radius. It is often expressed in terms of degree curve, D, corresponding to the degrees of arc subtended by a 100 foot chord at the track centerline. Mathematically,

$$D = (360/\pi)\sin^{-1}(50/R) \qquad (1)$$

where R is expressed in feet and D in degrees. The track superelevation or bank angle, φ_{se}, is the angle between the track and a horizontal plane. The curve radius, R, and superelevation angle, φ_{se}, are illustrated in Figure 1.

The track curvature, superelevation angle, and the vehicle forward speed, V, are commonly combined into a parameter of net lateral unbalance called the cant deficiency, φ_d, defined as

$$\varphi_d = V^2/(Rg) - \varphi_{se} \qquad (2)$$

where g is acceleration due to gravity. Cant deficiency represents an angular measure of lateral unbalance between centrifugal and gravitational forces. When $\varphi_d = 0$, the components of centrifugal force and vehicle weight parallel to the plane cancel each other and "balanced running" is achieved. In the United States, the allowable cant deficiency is limited to 6 degrees of inboard unbalance and 3 degrees of outboard unbalance [6].

The superelevation angle and cant deficiency can each be expressed in terms of equivalent inches of elevation of the outer rail (relative to the inner rail). Because a standard rail gauge is approximately 57 inches, the numerical value of superelevation or cant deficiency expressed in inches is quite close to the corresponding angle expressed in degrees.

In general, most lengths of track can be modeled using combinations of three types of track sections. These sections are tangent (straight) track, constant radius curved track, and transition spiral track. The transition spiral track connects tangent and constant radius curve track, and represents sections of curve entry and exit.

In this work, a simple model of deliberate track geometry is used [5]. In sections of tangent track, the track curvature and superelevation angle are zero. In sections of constant radius curve track, the curvature and superelevation angle are constants (and maximum). In transition spiral sections, the track curvature and superelevation angle are approximated by second order polynomial functions fitted between adjacent tangent and constant radius sections.

Unintentional Variations

Four irregularity degrees of freedom are commonly considered, corresponding to the vertical and lateral deviation of each rail relative to that rail's nominal (ideal) position [1]. Typically, these deviations are combined to give an alternative set of four independent irregularities: alignment, gauge, surface, and crosslevel. Alignment is the average of the lateral deviations of the two rails; gauge is the difference of the lateral deviations. Similarly, surface is the average of the vertical deviations of the two rails; crosslevel is the difference of the vertical deviations. Figure 2 is an illustration of the four irregularities, which are presented as four distinct modes of geometric deviation, analogous in a way to the different dynamic modes in a linear dynamic system. Actual irregularities may be considered to be a superposition of these four basic modes.

In general, unintentional variations, or irregularities, have both random and deterministic components. Random irregularities result from errors in rail manufacturing and installation; rail deformation occurs due to wear. Deterministic irregularities result from periodic phenomena such as rail joints (bolted or welded), and isolated transient track anomalies such as switches, turnouts, crossings and bridges [1].

The quality of the track is principally determined by the mean joint amplitude, the variances of the random irregularities and, to a limited extent, the spatial frequencies of the irregularities. In the United States, track quality is expressed in terms of track class. Six track classes are identified, class one being the worst (roughest) and class six being the best (smoothest) [2]. In the degraded or lower track classes, the rail joint component dominates, while for the better track classes (i.e., classes 4, 5 and 6) the stationary random process is most important.

[1] Alignment, crosslevel, gauge, and surface irregularities are defined in subsection Unintentional Variations.

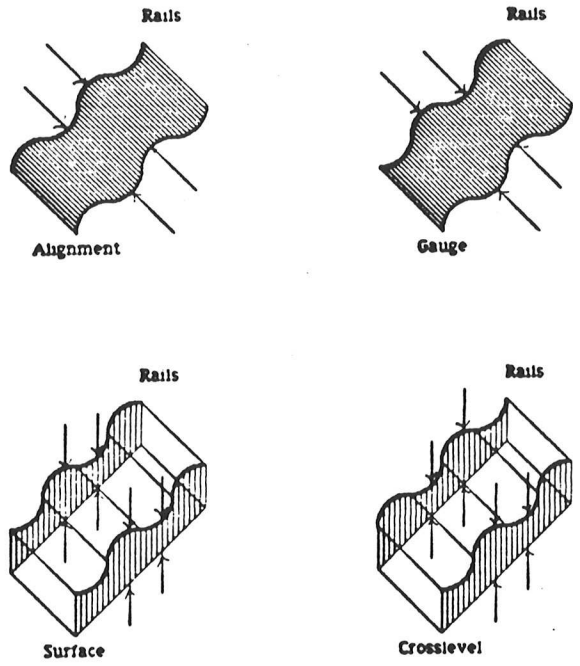

Figure 2: Irregularity Modes: Alignment, Gauge, Surface, Crosslevel.

Typically, rail joints are staggered between the left and right rails, with a rail length of 39 feet. The rail joint may be modeled as a cusp, damped sinusoid, or other form, occurring at regular intervals with its shape determined by its amplitude and some measure of its length [1]. In reality, the amplitude and length of the rail joints are not constant nor well determined. Thus, a better model of rail joint irregularities might be that of a periodically modulated random process in which the joint amplitude and length are stochastic processes, while the joint spacings are fixed.

Transient irregularities due to isolated phenomena also occur and may be modeled similarly. These irregularities are due to soft subgrade, poor drainage, and track construction. In addition to modeling realistic (i.e., field-encountered) irregularities, it is sometimes desirable to generate artificial irregularities. For example, sinusoidal irregularities of different frequencies may be used to determine vehicle frequency response to track inputs.

In this paper, particular attention has been paid to modeling typical rail irregularities as random processes. Alignment, gauge, and crosslevel irregularities are considered. Surface irregularities are neglected since the vehicle model used in this work is essentially a lateral model and surface irregularities primarily affect the vertical dynamics.

Generation of Random Irregularities. A standard tool used to model rail irregularities is the power spectral density. Functions that represent alignment, gauge, and crosslevel power spectral densities have been determined experimentally [2]. In this work, we have used functions obtained originally from Hamid, et al. [1] and have modified them, where necessary, to avoid differentiating white noise in the generation of irregularities.

The following equations have been used to represent single-sided power spectral densities for alignment, gauge, and crosslevel irregularities:

$$S_a(v) = A_a v_{a1}^2 / [v^2(v^2+v_{a1}^2)] \quad (3)$$

$$S_g(v) = A_g v_{g1}^2 / [(v^2+v_{g1}^2)(v^2+v_{g2}^2)] \quad (4)$$

$$S_c(v) = A_c v_{c1}^2 / [(v^2+v_{c1}^2)(v^2+v_{c2}^2)] \quad (5)$$

where S_a, S_g, and S_c are the alignment, gauge, and crosslevel power spectral densities, respectively, each measured in units of in^2/(cycle/ft); v is a spatial frequency in units of cycles/ft; v_{a1}, v_{g1}, v_{g2}, v_{c1} and v_{c2} are cutoff frequencies, also measured in cycles/ft; A_a, A_g and A_c are "roughness parameters" measured in units of in^2(cycle/ft). Values for these parameters for track classes one through six are given in Table 1.

Rail irregularities are generated from an appropriate power spectral density function. In general, equations (3), (4), and (5) can be written as:

$$S(v) = Av_1^2 / [(v^2+v_1^2)(v^2+v_2^2)] \quad (6)$$

Equivalently, these equations can be written as

$$S(v) = H(jv)S_i(v)H(-jv) \quad (7)$$

where H(jv) is

$$H(jv) = v_1 / [(v_1+jv)(v_2+jv)] \quad (8)$$

and $S_i(v)$ is an input power spectral density equal to the constant A. H(jv) represents the transfer function relating the frequency domain representation of an irregularity, Y(jv), and the input function, $Y_i(jv)$, i.e.,

$$Y(jv) = H(jv)Y_i(jv) = v_1 Y_i(jv) / [(v_1+jv)(v_2+jv)] \quad (9)$$

Rearranging,

$$v_1 Y_i(jv) = [v_1 v_2 + (v_1+v_2)jv + (jv)^2]Y(jv) \quad (10)$$

In terms of the Laplace variable, s, we have $s = j\omega = 2\pi jv$, $\omega_1 = 2\pi v_1$ and $\omega_2 = 2\pi v_2$ and thus, equation (10) becomes

$$2\pi Y_i(s/2\pi) = [\omega_1\omega_2 + (\omega_1+\omega_2)s + s^2]Y(s/2\pi) \quad (11)$$

We now define $Y_i(s/2\pi)$ and $Y(s/2\pi)$ to be the Laplace transforms of irregularities $y_i(x)$ and y(x), respectively, where the Laplace transformation involves integration over x. Assuming zero initial conditions, that is y(0) = y'(0) = 0, and taking the inverse Laplace transform of equation (11), we obtain the following differential equation in x relating $y_i(x)$ and y(x).

$$2\pi\omega_1 y_i(x) = \omega_1\omega_2 y(x) + (\omega_1+\omega_2)y'(x) + y''(x) \quad (12)$$

In theory, equation (12) may be integrated to obtain the irregularity, y(x), provided we know the input function, $y_i(x)$. However, since $y_i(x)$ has a constant power spectral density, it is a white noise signal [7].

A problem arises in attempting to solve equation (12) for y(x) using a numerical integration scheme due to the white noise input [7]. To eliminate this problem, we consider the original irregularity power spectral density to have most of its power below the frequency v_1 cycles/ft. That is, the "white" noise may be approximated as having a (single-sided) power spectral density equal to A for v between 0 and v_1, and equal to 0 for v greater than v_1. Then, the total power in the white noise is P, given by

$$P = Av_1 \quad (13)$$

This power is in units of $(\text{in-cycles/ft})^2$ and $y_i(x)$ is in units of in-cycles/ft. We can now integrate equation (12) numerically. The step size, X_s, should be selected such that $1/X_s$ is greater than $2v_1$ to avoid aliasing.

A random signal is described not only by its power spectral density, but also by some probability density function describing the relative frequency of occurrence of various signal amplitude levels. In this work, rail

irregularities are assumed to have Gaussian probability distribution functions. Arslan [2] argues that this is a reasonable approximation. In addition, the alignment, gauge, and crosslevel irregularities are assumed to be mutually independent [1]. The use of Gaussian irregularities is convenient in that a linear differential equation with a Gaussian forcing function will describe a Gaussian output function [8].

Thus, we can think of the white noise input function, $y_i(x)$, as being a Gaussian random process. For Gaussian processes with zero mean (a condition white noise meets), the total power, P, is given by

$$P = \sigma^2 \tag{14}$$

where σ^2 is the variance. Thus, to obtain $y(\dot{x})$ we can integrate equation (12) with zero initial conditions, step size X_s and input $y_i(x)$, where $y_i(x)$ is a sequence of independent random values having a Gaussian distribution with zero mean ($\mu = 0$) and variance given by

$$\sigma^2 = Av_1 \tag{15}$$

Sample Irregularities. The method described above was used to generate a number of sample rail irregularity profiles for a 500 ft tangent section of class 6 track. The resulting track alignment, gauge, and crosslevel irregularities are presented in Figures 3a, 4a, and 5a, respectively. These plots are too compressed to convey detailed information but provide a sense of the characteristics of typical irregularities, including the relative scales of the different deviations, as well as the rates of change and frequencies involved. Although they are random processes, the periodic nature of the rail irregularities should be noticed. The dominant frequencies are determined from the rail irregularity power spectral density cutoff frequencies (v_{a1}, v_{g1}, v_{g2}, v_{c1}, v_{c2}) listed in Table 1.

Table 1: Power Spectral Density Parameters (Units given in text).

	6	5	4	3	2	1
A_a	2.8×10^{-5}	5.0×10^{-5}	8.9×10^{-5}	1.6×10^{-4}	2.8×10^{-4}	5.0×10^{-4}
v_{a1}	5.6×10^{-2}	5.6×10^{-2}	5.6×10^{-2}	5.6×10^{-2}	5.6×10^{-2}	5.6×10^{-2}
A_g	2.8×10^{-5}	5.0×10^{-5}	8.9×10^{-5}	1.6×10^{-4}	2.8×10^{-4}	5.0×10^{-4}
v_{g1}	7.1×10^{-2}	7.1×10^{-2}	7.1×10^{-2}	7.1×10^{-2}	7.1×10^{-2}	7.1×10^{-2}
v_{g2}	8.3×10^{-3}	8.3×10^{-3}	8.3×10^{-3}	8.3×10^{-3}	8.3×10^{-3}	8.3×10^{-3}
A_c	3.4×10^{-5}	5.0×10^{-5}	7.4×10^{-5}	1.1×10^{-4}	1.6×10^{-4}	2.3×10^{-4}
v_{c1}	4.0×10^{-2}	4.0×10^{-2}	4.0×10^{-2}	4.0×10^{-2}	4.0×10^{-2}	4.0×10^{-2}
v_{c2}	7.1×10^{-3}	7.1×10^{-3}	7.1×10^{-3}	7.1×10^{-3}	7.1×10^{-3}	7.1×10^{-3}

From these simulated irregularities, power spectral densities were calculated numerically. The corresponding estimates of power spectral density are plotted (on linear scales) in Figures 3b, 4b, and 5b. These plots indicate the distribution of power of the (irregularity) signals as a function of spatial frequency, and reflect the relative concentration of signal power at the irregularity cutoff frequencies.

RAIL VEHICLE MODEL

The influence of geometric track variations on rail vehicle transient response is studied using a 42-state computer simulation model. As described in [4, 5], this model simulates the lateral (and yaw) dynamics of a rail transit vehicle operating on smooth tangent and curved track. This paper adds track irregularities as inputs to the vehicle model.

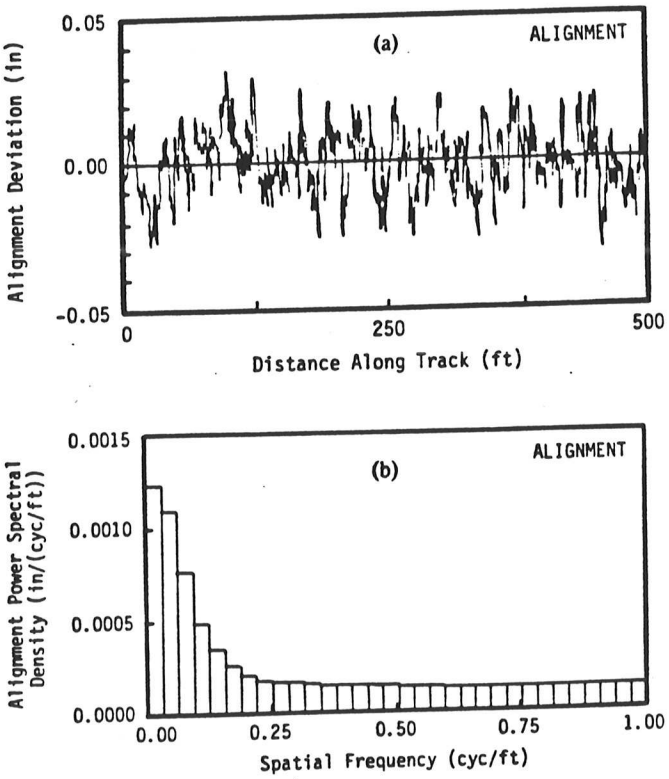

Figure 3: Alignment (a) Irregularity Profile, and (b) Power Spectral Density.

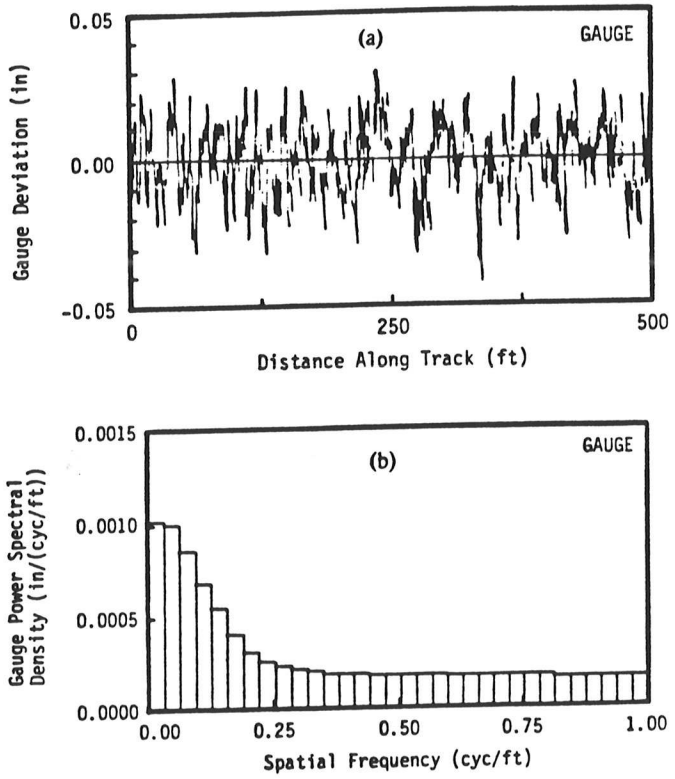

Figure 4: Gauge (a) Irregularity Profile, and (b) Power Spectral Density.

Track Model

A flexible rail model, which allows each rail to move in the lateral direction, is assumed. The rail is modeled as a lumped mass-spring-damper combination with effective lateral mass, viscous damping, and linear stiffness, respectively. Here, the lateral mass is assumed to be negligible. In addition to rail dynamic properties, track geometry variations, both deliberate and unintentional, as described above, are included and represent an important feature of the model.

Wheelset Model

Track geometry variations are transmitted to the rail vehicle through its wheelsets. A variety of wheel profile shapes are used by the transit industry. They may, in general, be classified as representing single-point contact or two-point contact profiles. In a single-point contact wheel profile, contact between the wheel and rail always occurs at only one "point" (actually a "patch") on the tread or flange. In contrast, a two-point contact wheel profile is characterized by the possibility of wheel/rail contact which occurs at two separate points, one on the tread and one on the flange. For the simulation results in this paper, wheelsets with two-point contact profiles corresponding to new AAR 1 in 20 wheels on worn rail are assumed.

For a wheelset negotiating curved and/or irregular track, slip or creepage may develop at the rails. Normal forces acting on the slipping wheelset result in the generation of friction-type forces known as creep forces. Kalker [9] has developed linear, simplified nonlinear, and exact nonlinear theories to predict these contact-patch creep forces. We have adopted a model that includes the linear Kalker theory for small creepages and saturates at the adhesion limit for larger creepages [4, 5]. This model appears to agree very closely with Kalker's more sophisticated nonlinear theories [10].

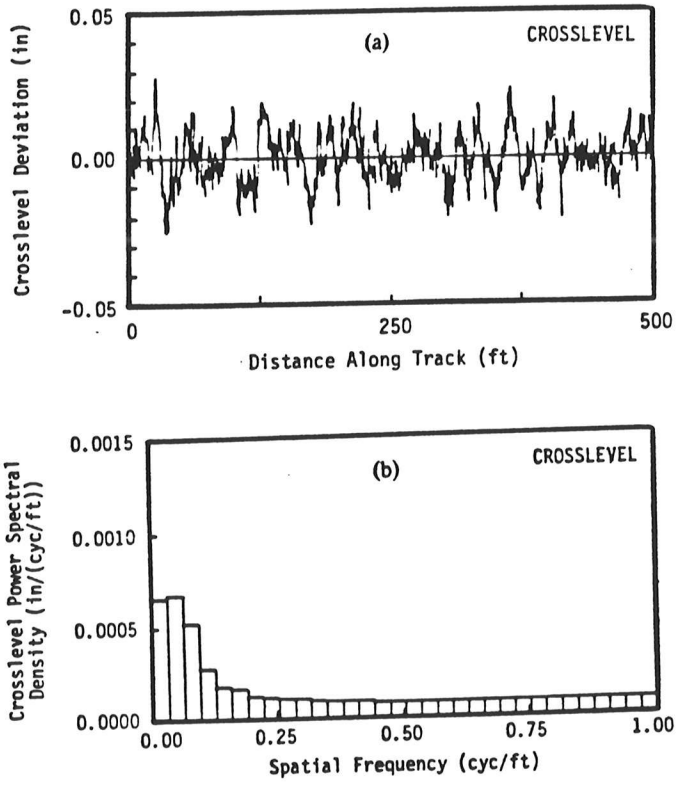

Figure 5: Crosslevel (a) Irregularity Profile, and (b) Power Spectral Density.

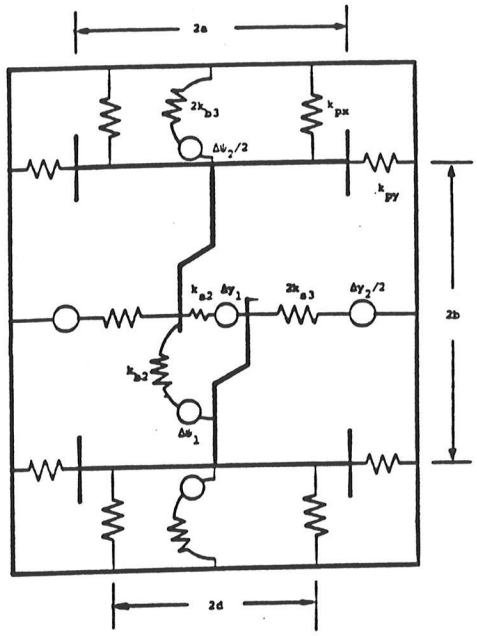

Figure 6: Generic Truck Model.

Vehicle Model

A rail transit vehicle consists of a carbody supported by four wheelsets, two truck frames, and two bolsters. The wheelsets are connected to the truck frame through the primary suspension. Each bolster sits on a truck frame and is connected to the carbody through the secondary suspension.

The rail vehicle model consists of rigid-body inertial elements connected by parallel spring/damper combinations representing the suspension characteristics. A general truck model, representing a variety of suspension designs, including conventional trucks and various self and force steered configurations, has been developed and is shown in Figure 6. Details of the rail vehicle model are presented in [4, 5].

The effects of track geometry variations on vehicle behavior may be interpreted as modifications to the dynamic equations of the vehicle model operating on smooth, tangent track. The deliberate variations (curvature and superelevation) manifest themselves at each wheelset in the matrix transformation between the wheelset reference frame and an inertially fixed frame. The crosslevel irregularity is considered an addition to the superelevation. Alignment and gauge irregularities are taken into account as offsets in the wheelset lateral equations.

Performance Indices

Vehicle dynamic behavior is represented by trajectories of state variables, including wheelset, truck, and carbody excursions, angles, and their rates. Certain performance indices are represented by, or calculated from, these trajectories for the purpose of quantitative comparison of different vehicle/track configurations. For instance, some of the indices calculated from state trajectories are associated with energy consumption, and include losses due to contact patch work and suspension dissipation[2].

SIMULATIONS

This section presents sample results of dynamic simulations which were conducted using the general track geometry model as input to the vehicle model. The vehicle was modeled with unsteered truck suspensions, and parameters typical of conventional rail transit vehicles [4, 5]. In addition, laterally flexible rails with linear rail damping were assumed. For the simulations, the vehicle dynamic equations were integrated numerically

[2] Journal bearing losses also represent a performance index, and are discussed in [11].

using a double-precision, fourth-order Runge-Kutta scheme with variable time-step. The time-step was 0.0006 sec when tread contact occurred at all wheel/rail interfaces. When flange contact occurred at any wheel, the time-step was automatically reduced to 0.0004 sec. The computer time required on a DEC VAX 11/750 was approximately 8-10 CPU minutes for a 1 sec simulation.

Dynamic Curving

The simulation results presented in this subsection represent right-hand curve entry on smooth track (no irregularities). The following assumptions were made: (1) The vehicle enters 50 ft of tangent track at the initial time (t = 0 sec) from a centered tangent track position. (2) Following the tangent track, the vehicle enters a 150 ft transition spiral curve into constant radius curve track. (3) The vehicle operates at a constant forward speed of 50 ft/sec (34 mph). (4) The superelevation angle is chosen to give zero cant deficiency (in the constant radius section). (5) The lateral rail stiffness is 1.0×10^6 lb/ft. (6) The wheel/rail coefficient of friction is 0.3.

Simulation results of curve entry into 0.0, 2.5, 5.0 and 10.0 degree curves are presented. (Note that the first case represents tangent track only and is not strictly "curve entry".) Figure 7a shows the net lateral excursion (relative to the left rail) of the leading wheelset as a function of time. For negotiation of tangent track, the leading wheelset does not deviate from its nominal centered position. For entry into a 2.5 degree curve, the leading wheelset exhibits oscillation as the flange of its outer wheel moves toward the rail, but never reaches it. For the 5.0 and 10.0 degree curve entry cases, the leading outer wheel exhibits flanging. The net lateral excursion is limited by the wheelset flange clearance (in this case, 0.32 in).

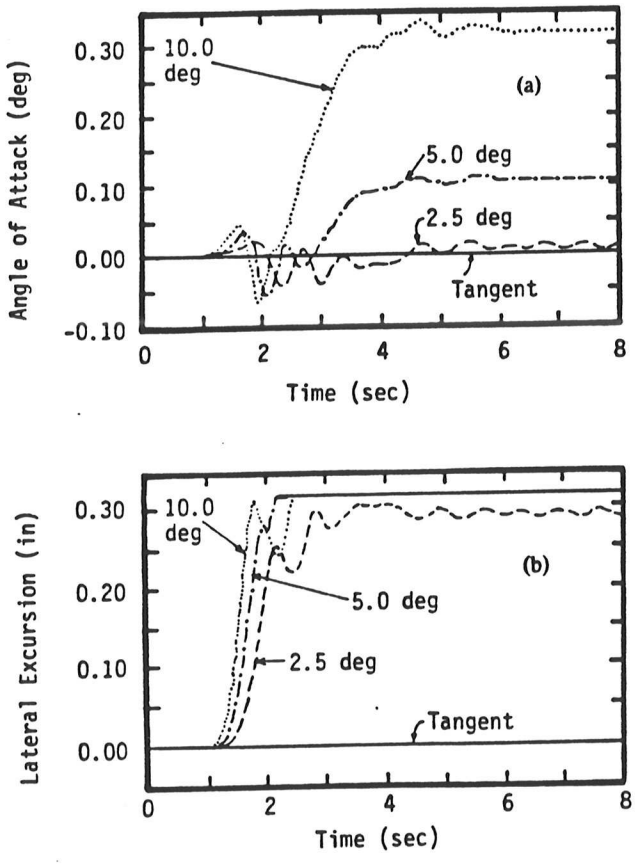

Figure 7: History of Leading Wheelset (a) Lateral Excursions, and (b) Angles of Attack of a Conventional Vehicle with New AAR Wheels Negotiating a 150 ft Curve Entry Spiral into 0.0, 2.5, 5.0 and 10.0 deg Curves.

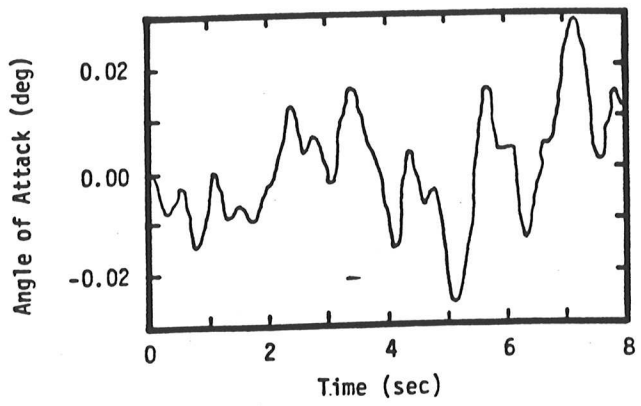

Figure 8: History of Leading Wheelset Angle of Attack of a Conventional Vehicle with New AAR Wheels Negotiating Class 6 Tangent Track.

The yaw angle of the leading wheelset is shown in Figure 7b. As above, for negotiation of tangent track, the yaw angle of the leading wheelset does not deviate from its nominal position. In each of the other three cases, the wheelset moves with some oscillation to a steady-state attack angle. The magnitude of this angle depends on the severity of the final degree curve, and is larger for the sharper curves.

Irregularity Effects

This subsection addresses vehicle behavior on tangent, irregular track. The runs simulate conventional vehicle behavior on tangent track of different quality (smooth, class six, class five, and class four) at different speeds (from 30 to 70 ft/sec, ie., 20 to 48 mph). Figure 8 is a plot of yaw angle (angle of attack) of the leading wheelset versus time for a conventional vehicle operating at 50 ft/sec (34 mph) on class 6 tangent track. The plot exhibits a yaw oscillation about the centered position due to the irregularity inputs. In contrast, on smooth track the angle of attack remains zero.

Since the track irregularities are random processes, the outputs can also be viewed as random processes and be treated as statistical quantities. The total vehicle dissipation (power) as a function of time was calculated and used to determine the ***mean*** total vehicle dissipation. The mean or average power on tangent track is shown as a function of vehicle forward speed and track class in Figure 9. The power increases with both speed and track class. The increase observed on class 4 track at 50 ft/sec is believed to be due to resonance in the rails. Clearly, random track irregularities represent a significant vehicle input.

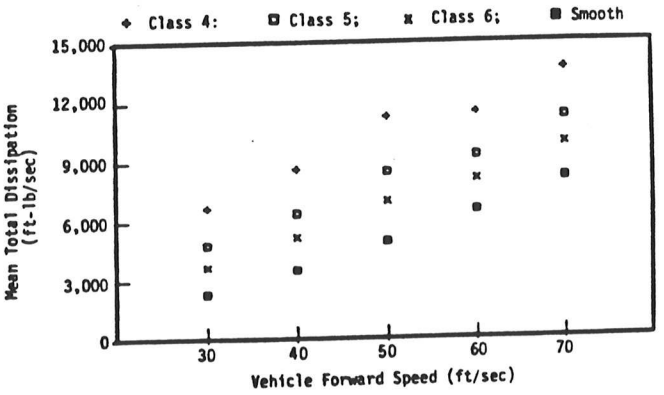

Figure 9: Average Total Dissipation for Conventional Vehicle with New AAR Wheels Negotiating Tangent Track as a Function of Speed and Track Class.

Dynamic Curving and Irregularity Effects

The performance of vehicles operating on curved irregular track was studied. The nature of curve entry dynamics[3] on unsmooth track is shown in the response of a conventional vehicle with new AAR wheels running into a 2.5 degree curve with class 6 track irregularities. Figures 10a and 10b show the leading wheelset lateral excursion and angle of attack, respectively, as a function of time. The leading wheelset initially displaces inward. As the front truck enters the spiral curve, the wheelset moves toward the outer rail, but exhibits substantial oscillations. In contrast to its response on smooth track (see Figure 7), the wheelset angle of attack also displays significant oscillations. The wheelset does not attain steady-state values of lateral excursion or yaw angle due to the irregularities. The ability to study the combined effect of track curvature, superelevation, and track irregularities represents an important advantage of the simulation model.

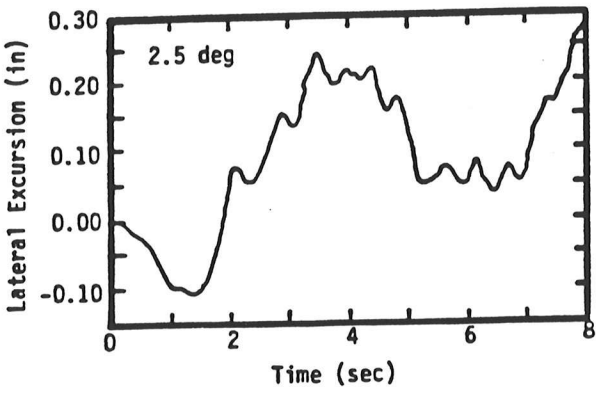

(a)

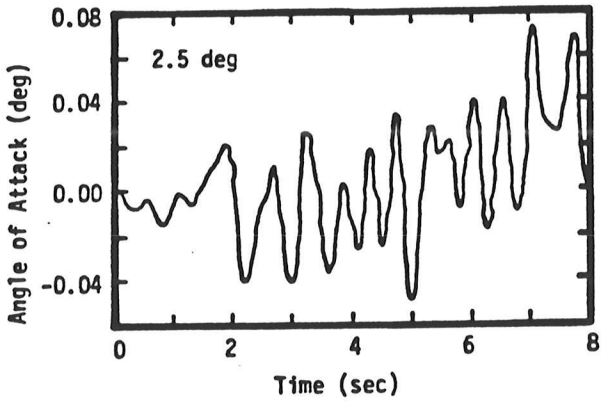

(b)

Figure 10: History of Leading Wheelset (a) Lateral Excursion, and (b) Angle of Attack of a Conventional Vehicle with New AAR Wheels Negotiating a 150 ft Curve Entry Spiral into a 2.5 deg Curve with Class 6 Irregularities.

[3]The assumptions described in subsection Dynamic Curving apply.

CONCLUSIONS

Whether deliberate or unintentional, deviations in rail geometry from smooth tangent track represent an important input to the vehicle system. This paper presents the development of a general model of track geometry variations. The model is used to generate input data for a rail vehicle dynamic simulation model. Limited results are presented and are intended to demonstrate the value of the general rail geometry model for studies of rail vehicle response and performance. Currently, we are using the model described here to study in depth the influence of track geometry variations on vehicles with different suspension designs and wheel profiles. Results of these studies will be reported separately.

ACKNOWLEDGMENTS

Support for the work described here was provided in part by the Department of Mechanical Engineering, Carnegie-Mellon University, Pittsburgh, PA.

REFERENCES

1. Hamid, A., Rasmussen, K., Baluja, M., and Yang, T.L., "Analytical Descriptions of Track Geometry Variations," U.S.D.O.T., Federal Railroad Administration, December 1983.

2. Arslan, V.A., "The Application of Statistical Linearization to Nonlinear Rail Vehicle Dynamics," Ph.D. Thesis, Dept. of Mechanical Engineering, M.I.T., May 1980.

3. Dzielski, J.E., "Modeling and Simulation of Freight Car Energy Dissipation Due to Vehicle/Track Dynamics," M.S. Thesis, Dept. of Mechanical Engineering, M.I.T., June 1984.

4. Nagurka, M.L., "Curving Performance of Rail Passenger Vehicles," Ph.D. Thesis, Dept. of Mechanical Engineering, M.I.T., May 1983.

5. Nagurka, M.L., Wormley, D.N., and Hedrick, J.K., "Dynamic Curving Performance of Rail Transit Vehicles," ASME Technical Paper 84-WA/DSC-12, presented at the 1984 ASME Winter Annual Meeting, New Orleans, December 1984.

6. Bell, C.E., "Curving Mechanics of Rail Vehicles," Ph.D. Thesis, Dept. of Mechanical Engineering, M.I.T., September 1981.

7. Stearns, S.D., *Digital Signal Analysis*, Hayden Book Company, Inc., Rochelle Park, New Jersey, 1975.

8. Bertsekas, D.P., *Dynamic Programming and Stochastic Control*, Academic Press, New York, 1976.

9. Kalker, J.J., "Survey of Wheel-Rail Rolling Contact Theory," *Vehicle System Dynamics*, Vol. 5, 1979, pp. 317-358.

10. Shen, Z.Y., Hedrick, J.K., and Elkins, J.A., "A Comparison of Alternative Creep Force Models for Rail Vehicle Dynamic Analysis," *Proceedings of the 8th IAVSD Symposium*, M.I.T., Cambridge, MA, August 15-19, 1983, pp. 591-605.

11. Bernsteen, S.A., "A Theoretical Analysis of the Rolling Resistance of Railway Vehicles from Fundamental Mechanics," Ph.D. Thesis, Dept. of Physics, Carnegie-Mellon University, 1979.